Journal of Power Sources 249 (2014) 13–20

Contents lists available at ScienceDirect

Journal of Power Sources

journal homepage: www.elsevier.com/locate/jpowsour

High performance zinc air fuel cell stack

Pucheng Pei*, Ze Ma, Keliang Wang, Xizhong Wang, Mancun Song, Huachi Xu

State Key Lab. of Automotive Safety and Energy, Tsinghua University, Beijing 100084, China

HIGHLIGHTS

- A ZAFC system with MnO_2 as catalyst and KOH electrolyte was developed.
- The peak power density of ZAFC can be as high as 435 mW cm^{-2}.
- The influence factors on cell performance and uniformity are studied.
- The dynamic response time of ZAFC is in milliseconds.

ARTICLE INFO

Article history:
Received 17 July 2013
Received in revised form
15 October 2013
Accepted 17 October 2013
Available online 29 October 2013

Keywords:
Zinc air fuel cell
Electrolyte circulation
Uniformity
Dynamic response

ABSTRACT

A zinc air fuel cell (ZAFC) stack with inexpensive manganese dioxide (MnO_2) as the catalyst is designed, in which the circulation flowing potassium hydroxide (KOH) electrolyte carries the reaction product away and acts as a coolant. Experiments are carried out to investigate the characteristics of polarization, constant current discharge and dynamic response, as well as the factors affecting the performance and uniformity of individual cells in the stack. The results reveal that the peak power density can be as high as 435 mW cm^{-2} according to the area of the air cathode sheet, and the influence factors on cell performance and uniformity are cell locations, filled state of zinc pellets, contact resistance, flow rates of electrolyte and air. It is also shown that the time needed for voltages to reach steady state and that for current step-up or current step-down are both in milliseconds, indicating the ZAFC can be excellently applied to vehicles with rapid dynamic response demands.

1. Introduction

Environmental pollution and shortage of fossil fuels have made it a popular trend to develop electrical vehicles (EVs) and use renewable energy. Many efforts are focused on batteries and fuel cells, which can be used for EVs propulsion and large-scale energy storage. However, the existing batteries and hydrogen fuel cells cannot meet all the market needs; for example: low price, high safety, longer lifetime, and zero pollution. For electrochemical power sources, it is worth noting that zinc possesses a unique set of characteristics as anode material, including low equilibrium potential, electrochemical reversibility, stability in aqueous electrolytes, good conductivity, low equivalent weight, high specific energy, and high volumetric energy density [1–4]. Moreover, zinc also has other merits, such as, abundant resources, low cost, low toxicity, easy storage and safe handling. Up to now various types of zinc air batteries and fuel cells have been developed, such as primary battery [5], electrically rechargeable battery [6–8] and fuel cell (or called mechanically rechargeable battery) [9–12]. However, the primary battery is not applicable to EVs and energy storage, and the electrically rechargeable battery has a relatively short lifetime [13]. Compared to the hydrogen proton exchange membrane fuel cell (PEMFC) [14], the catalysts of zinc air fuel cell (ZAFC) are made by non-precious metals and also the zinc fuel is convenient for storage and transportation [11,15,16]. Additionally, the high stability of zinc in aqueous electrolytes makes the ZAFC more superior to the high energy lithium ion battery in safety. Overall, the ZAFC has great potential for EVs propulsion and large-scale energy storage, and is also attractive for portable, stationary, and military purposes.

Currently, the performance of ZAFC still cannot meet the commercialization requirement. The power densities of ZAFC with manganese dioxide (MnO_2) catalyst reported in previous researches are quite low, mostly in the range of 50–100 mW cm^{-2} [17–19]. This falls far behind the PEMFC. MnO_2 is one of the typical oxygen reduction catalysts, and has a reasonably high catalytic activity for oxygen reduction in alkaline electrolyte. In this study, a ZAFC stack with inexpensive MnO_2 catalyst was developed to study the factors affecting the stack performance and maximize power density.

* Corresponding author. Tel./fax: +86 10 62788558.
E-mail address: pchpei@mail.tsinghua.edu.cn (P. Pei).

0378-7753/$ – see front matter © 2013 Elsevier B.V. All rights reserved.
http://dx.doi.org/10.1016/j.jpowsour.2013.10.073

2. Experimental

2.1. Stack design and assembly

The development of a zinc air fuel cell with a configuration of bipolar plates in series is shown in Fig. 1. The bipolar design allowed current to flow from the anode to the adjacent cathode with minimal electrical resistance. The anode plate, cathode plate, and bipolar plates were fabricated from graphite material, and each fuel cell had an active surface area of 215 cm^2. The air cathode was constructed of three layers: an active layer, a current collector layer, and a hydrophobic layer (as shown in Fig. 1). The active layer was produced from a mixture of active carbon powder with manganese oxide catalyst powder and PTFE binder. The current collector layer was a woven nickel mesh. The hydrophobic layer was a porous Teflon film. The configurations of the anode chamber are shown in Fig. 2. At the bottom of the zinc pellet beds was a gap or mesh layer that allows potassium hydroxide (KOH) electrolyte and the extremely small particles to fall out of the pellets bed.

The chemical reactions taking place in the ZAFC stack and the transportation of electrons in a bipolar plate can be summarized as Fig. 1. During the power generation process, Zinc lost electrons to the graphite plate turning to a Zn^{2+} cation. The electrons generated on the anode traveled via the bipolar plate to an air cathode where the reduction of oxygen took place forming hydroxyl ions (OH^-). The hydroxyl ions traveled towards the anode side via the electrolyte and combined with zinc cations to form zinc oxides. Because the hydrophobic layer was insulated, the electrons, generated in the anodes and traveling via the bipolar plates, could only be transported from the air cathode margins into the active layer and the current collector layer, as shown in Fig. 1. In order to connect the circuit between the bipolar plates and air cathodes, nickel foils (0.08 mm thick) were used to edge-clad the air cathode sheets (see Fig. 3).

Fig. 4 shows a schematic design of the zinc air fuel cell system. Zinc pellets with an average size of 1 mm stored in the fuel tank, were fed to each anode chamber uniformly and intermittently by a mechanical device above the fuel cell stack. Potassium hydroxide (KOH) electrolyte (40 wt.%) was contained in a separate storage tank, and the electrolyte was driven by a magnetic pump to make circulation flow. Under the action of gravity, the zinc pellets automatically entered the anode chamber trough from the upper slit with the flowing electrolyte. The discharge products (potassium zincate) were carried out by the flowing electrolyte. Meanwhile, the ambient air was fed through the stack inlet and distributed in parallel amongst the unit cells by an electric fan. The outflow from the unit cells were combined in the outlet header and exited through the stack outlet. Similar to the traditional hydrogen fuel cell system, the fuel tank or the energy reservoir can be scaled up independently of the power.

2.2. Stack testing

At first, a 5-cell stack with anode chamber of type V was assembled and the polarization characteristics of each cell were tested, and the cells located from the positive electrode (near to the blower) to negative electrode were numbered #1, #2, #3, #4, and #5 in turn. Then several 2-cell stacks were assembled, and series of control tests were carried out to study the effects of different cases on performance differences between cells in the 2-cell stack. The cases are shown in Table 1. In the 2-cell stack, the cell located close to the blower was numbered #1, and the other cell was numbered #2. All of the air cathode sheets used in 5-cell and 2-cell stacks were cut from a large one. Only the air cathode A and B were used twice in Case I and Case II. The edge-cladding material for air cathode was nickel foil. The corroded nickel foils were exposed to room air for more than a month, while the cleaned nickel foils were treated ultrasonically with 1 mol L^{-1} HNO_3 and 1 mol L^{-1} HCl, and then washed with deionized water. In order to eliminate the effect of the changes of zinc pellets size and electrolyte concentration after the tests on the performance of ZAFC, the zinc pellets and the KOH electrolyte used in the 5-cell stack and 2-cell stack tests were changed with fresh ones before each tests. Besides, in all of the tests, the amounts of KOH electrolyte were the same, and the flow rates of electrolyte and air were kept constant.

In addition, the dynamic response characteristics of ZAFC were tested with the 2-cell stack used in Case IV. In order to investigate the step-up characteristics, the current of the stack was firstly stabilized at 10 A, then followed by loading the current to 20 A, 30 A, 40 A, 50 A, respectively, with stack voltage monitored and recorded. Also, current step-down cases were performed, in which the stack was firstly stabilized at 20 A, 30 A, 40 A, 50 A, then stepped down to 10 A, respectively.

All of the experiments were implemented at room temperature, and the change of relative humidity of ambient air was negligible. An electronic load (Hoecherl & Hackl GmbH ZLSV1502) was used for the performance tests, and a NI PXI-1033 data acquisition instrument was used to measure each cell voltage.

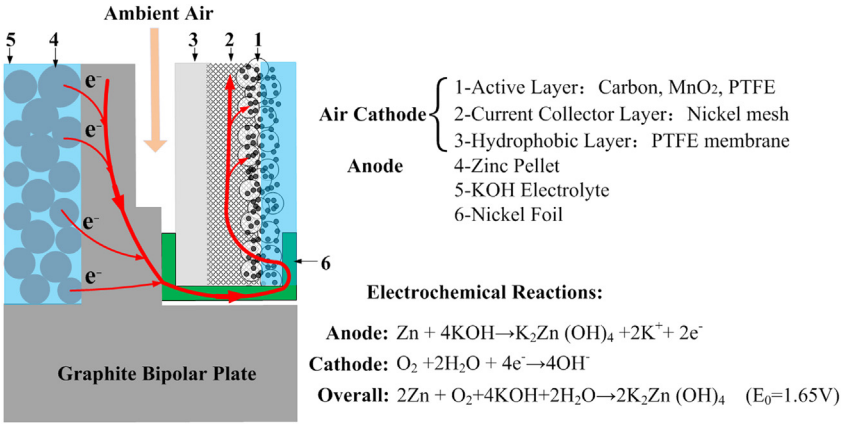

Fig. 1. Basic principle of ZAFC.

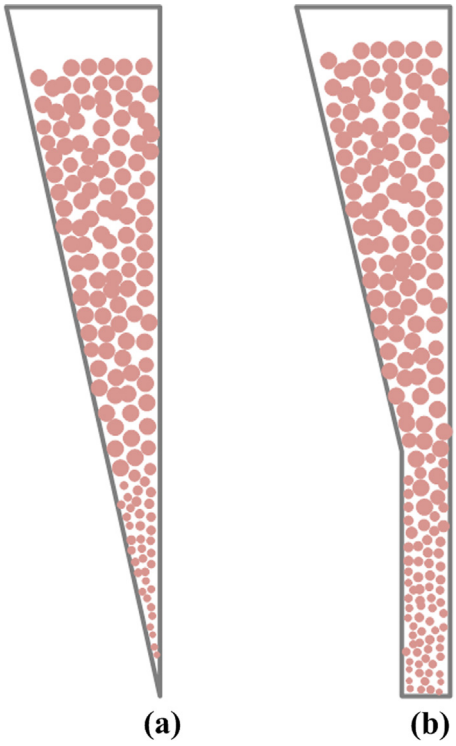

Fig. 2. (a) anode chamber of type V and (b) anode chamber of type Y.

3. Results and discussion

3.1. Polarization characteristics of 5-cell stack

In a trial test, the performances of each cell in the 5-cell stack are plotted in Fig. 5. The results show that the peak power of the stack with five cells is 138 W. The performances of the center fuel cells are relatively better than those on both sides of the stack. The peak power density of #3 cell is 182 mW cm^{-2} at 0.87 V, while the current density at the peak power point is 209 mA cm^{-2}.

The result of the 5-cell stack test indicates that the center fuel cells are more outstanding on polarization characteristic than those on both sides of the stack. This phenomenon also existed in PEMFC stacks [20–22], and one of the major reasons is the nonuniform distribution of temperature in the stack. The temperatures of the cells on both sides of the stack are relatively lower for better heat dissipation. According to previous studies, the polarization characteristic of ZAFC increases with the temperature [19], which confirms the fact that the center fuel cells of the stack have better performances in higher temperatures.

3.2. Polarization and constant current discharge characteristics of 2-cell stack

3.2.1. Effect of the location of single cell

Fig. 6 presents the polarization performances of each single cell of the 2-cell stack in Case I and Case II. The results show that the performances of cells in the 2-cell stack are similar to the cells on both sides of the 5-cell stack, but slightly degraded. Both the power of #1 cell of the 2-cell stack in Case I and Case II are lower. Constant current discharge characteristics of the cells in Case I and Case II are depicted in Fig. 7. Note that the concentration of the potassium zincate in the electrolyte increases with the time of discharge, while the concentration of hydroxide decreases, therefore the voltages of the cells during constant current discharge decrease gradually. Meanwhile, both the characteristics of polarization and constant current discharge of #2 cell are better than that of #1 cell, as shown in Figs. 6 and 7.

It can be considered that the temperature difference between the two cells of a 2-cell stack is negligible, but the performance differences still exist. Meanwhile, the results of Case I and Case II confirm that the performance differences between the two cells are not caused by air cathodes. Therefore, it can be inferred that the location of cell has an effect on the performance of ZAFC stack, especially the position of the intake blower. As the inlet and outlet manifold flows are perpendicular to the gas flow through the channels on the electrodes, the different location of single cell would get nonuniform flow distribution.

3.2.2. Effect of filled state of zinc pellets

The filled state of zinc pellets in a cell affects the active area and the ohmic resistance of the anode and in turn affects the performance of fuel cell significantly. And the filled state of zinc pellets is determined by the configuration of anode chamber. Fig. 8 gives the performances of each single cell in Case I and Case III. The results show that the polarization characteristics improved significantly

Fig. 3. Edge-cladded air cathode with nickel foils.

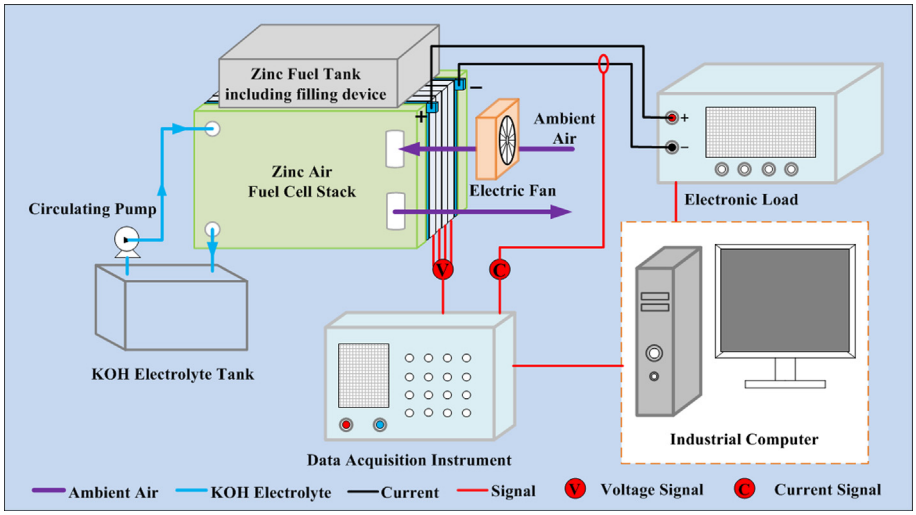

Fig. 4. Zinc air fuel cell system.

Table 1
Cases of the 2-cell stack.

Case	Air cathode of cell #1	Air cathode of cell #2	Configuration of anode chamber	Edge-cladding material
I	Air cathode A	Air cathode B	Type V	Corroded nickel foil
II	Air cathode B	Air cathode A	Type V	Corroded nickel foil
III	Air cathode C1	Air cathode C2	Type Y	Corroded nickel foil
IV	Air cathode D1	Air cathode D2	Type Y	Cleaned nickel foil

after the anode chamber configuration was modified from type V to type Y. The peak power density of #2 cell in Case III is as high as 274 mW cm^{-2} at 0.63 V, when the current density of the peak power point is 420 mA cm^{-2}.

The zinc filled state may be the main reason for performance difference in Case I and Case III. According to"1/3 bridging rule" [23], when the gap/particle size ratio is smaller than three, a particle bridging phenomena tends to occur and prevents the particles from dropping into the bottom of the gap. After tests of Case I and Case III, zinc filled state in anode chambers were studied by disassembling the stacks, as shown in Figs. 9 and 10. It can be found that the bottom portion of type V anode chamber is not filled with zinc pellets, resulting in sharp decrease of the affective active area of anode. Meanwhile, the zinc pellets filled in the type Y anode chamber are much more homogeneous, and the inactive region is reduced to a minimum.

3.2.3. *Effect of contact resistance*

Fig. 11 presents the polarization curves of each single cell in Case III and Case IV with different edge-cladded materials for the air cathode. The results show that the polarization characteristic improved significantly after the edge-cladded material was changed from corroded nickel foil to cleaned nickel foil. In Case IV, the peak power of 2-cell stack is 160 W, especially the peak power density of #2 cell is as high as 435 mW cm^{-2} at 0.86 V, and the current density of the peak power point is 510 mA cm^{-2}.

A fuel cell stack suffers from voltage losses, which primarily originate from three sources: activation polarization, ohmic polarization and concentration polarization. And the ohmic resistance of the cell is due to the resistance to flow of ions in the electrolyte, resistance of the stack materials and various contact resistances. Based on the calculation results from the polarization

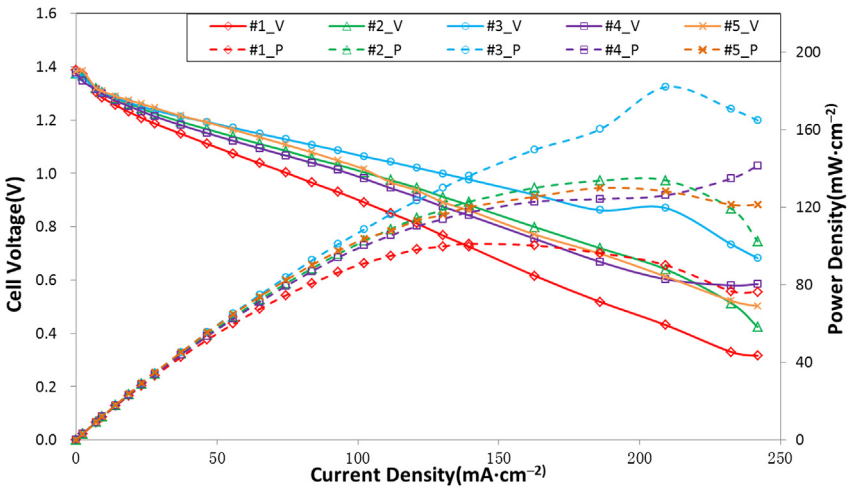

Fig. 5. Polarization characteristics of each cell of a 5-cell stack.

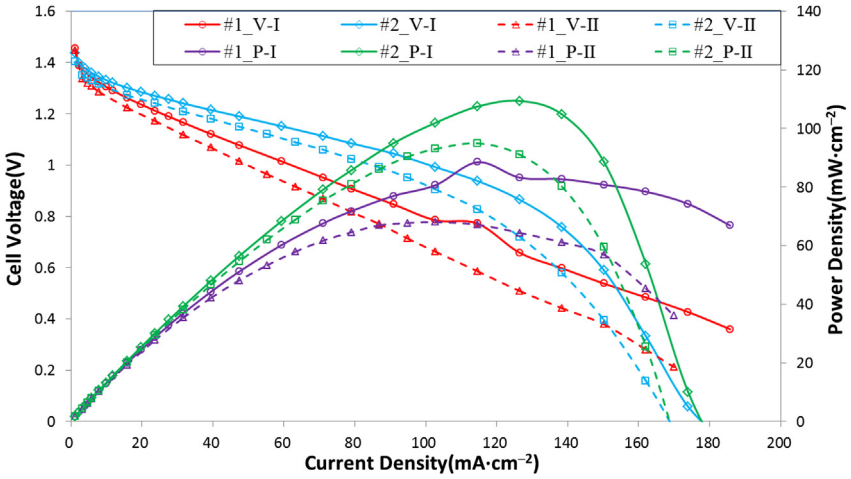

Fig. 6. Polarization characteristics in Case I and Case II.

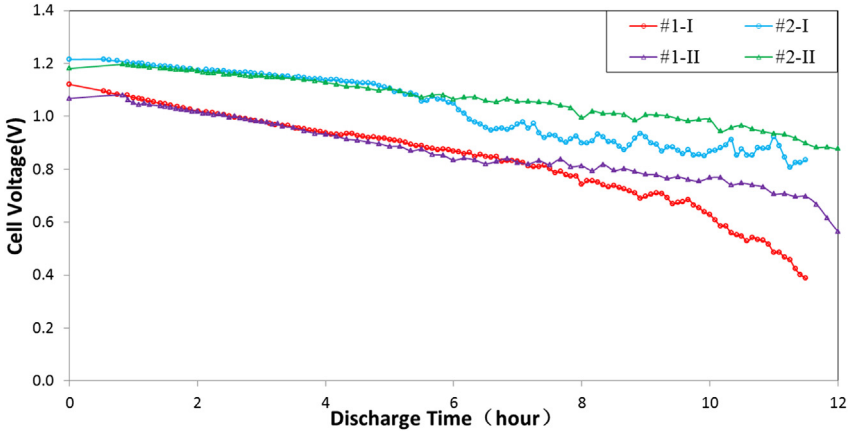

Fig. 7. Constant current discharge (46 mA cm^{-2}) characteristics in Case I and Case II.

characteristics of Case III and Case IV (Fig. 11), the ohmic resistance of #2 cell in Case III is 1.56 Ω cm^2, which is twice the ohmic resistance 0.77 Ω cm^2 of #2 cell in Case IV. Therefore, it can be deduced that removing the oxide film from the surface of nickel foil can significantly decrease the contact resistance, and improve the performance of the stack. Unlike the air cathode used in the traditional PEM fuel cell, in which conductive diffusion layer (carbon paper) can transport current into bipolar plates directly within the whole surface, the air cathode used in present ZAFC is inconvenient for current transportation. Therefore, it is particularly important to develop face conductive air cathodes and to minimize the contact resistance of ZAFC stacks.

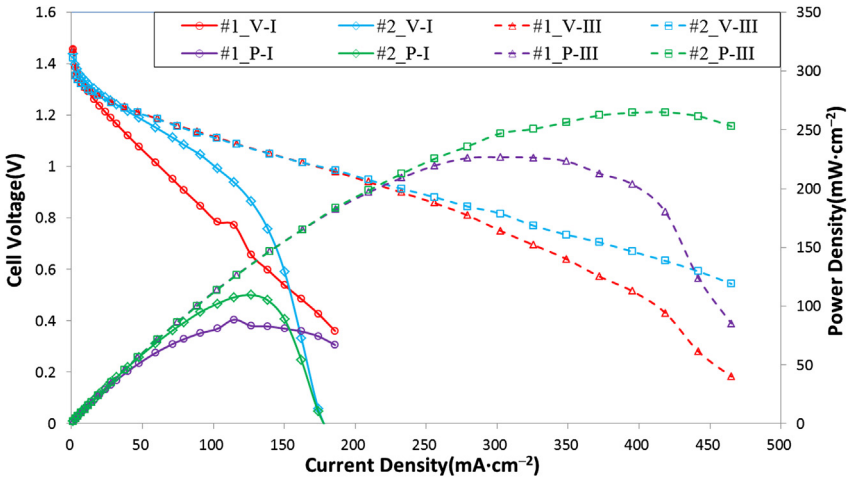

Fig. 8. Polarization characteristics in Case I and Case III.

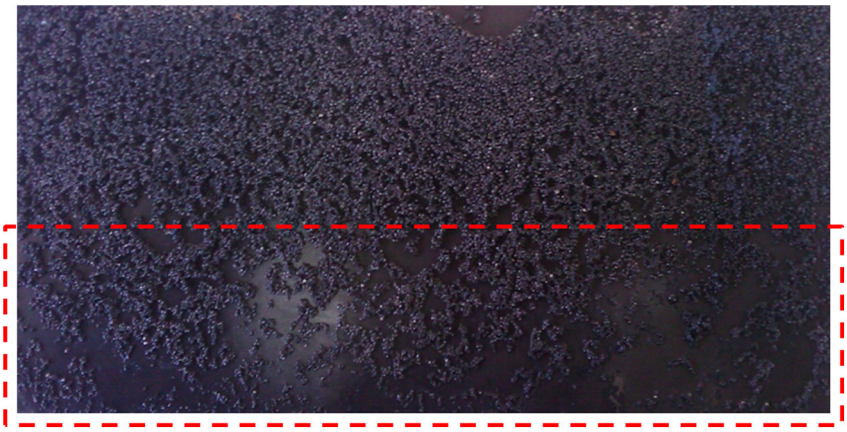

Fig. 9. Zinc pellets filled in type V anode chamber in Case I.

Fig. 10. Zinc pellets filled in type Y anode chamber in Case III.

3.2.4. Effect of the flow state of electrolyte and air

As shown in Fig. 10, the white mass on zinc pellets surface in the red section (in web version) is zinc oxide. It indicates that electrolyte flow rate was too slow in that region, and confirms that the insufficient electrolyte flow is one of the reasons for concentration polarization in ZAFC. By the fuel cell polarization theories, at high current conditions, the concentration polarization is caused by the depletion of electroactive materials on the electrode surface. For

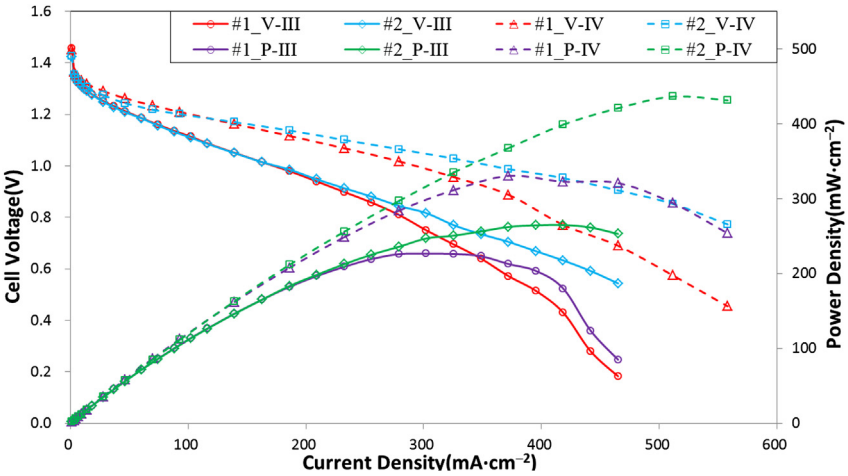

Fig. 11. Polarization characteristics in Case III and Case IV.

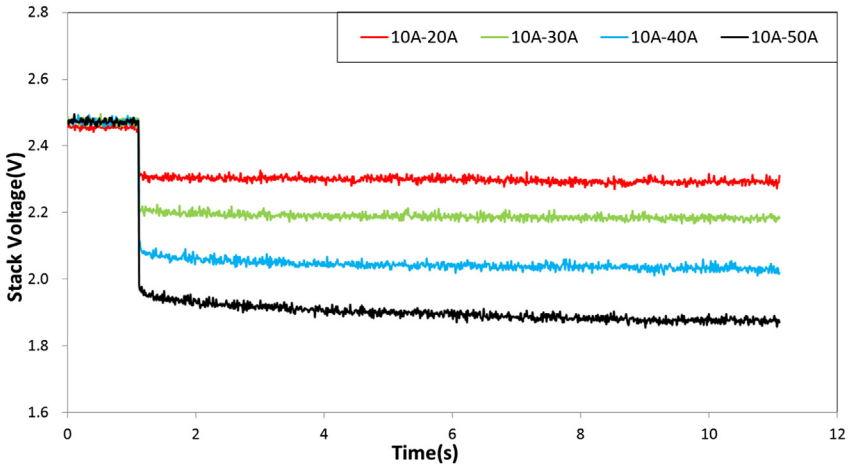

Fig. 12. Current step-up characteristics of 2-cell stack.

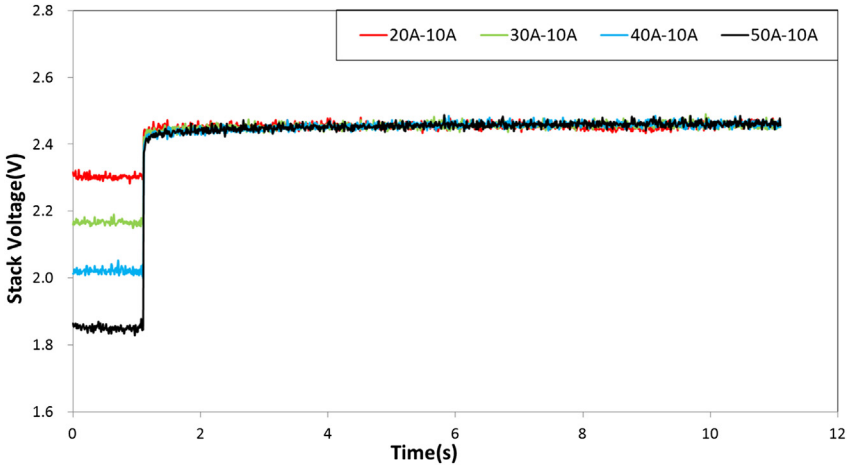

Fig. 13. Current step-down characteristics of 2-cell stack.

the ZAFC, the concentration polarization may be caused by the depletion of KOH or oxygen. Accordingly, the KOH electrolyte flow rate should be sufficient to provide hydroxide ions at such a rate as matches the reaction stoichiometry on the surface of the zinc particles and removes the reaction product away. Clearly, if the electrolyte flow rate cannot meet the conditions given above, zinc oxide will be formed in preference to potassium zincate. In addition, non-optimized air supplying may lead to nonuniform air distribution for different cells, also contributing to concentration polarization at high current conditions.

3.3. *Dynamic response characteristic*

The dynamic performance of fuel cell is one of the important criteria for automotive application. The step-up and step-down characteristics of the 2-cell ZAFC stack in Case IV are depicted in Figs. 12 and 13. The test results show that the dynamic response characteristics of stack voltage responding to both current step-up and current step-down are excellent. Time needed for voltages to reach steady state is in milliseconds, and hardly changes with the step amplitude. Moreover, compared to PEMFCs [24,25], the voltage overshoot and undershoot behaviors never take place on the ZAFC while load changes rapidly. This indicates that ZAFC is applicable to those applications including automobiles where dynamic response is crucial.

4. Conclusion

A zinc air fuel cell stack was designed and manufactured with potassium hydroxide electrolyte circulation flow. From tests of a 2-cell stack in 4 cases and a 5-cell stack, conclusions are drawn as follows:

1. The peak power density of the ZAFC, with MnO_2 as the catalyst, can reach 435 mW cm^{-2} (at 0.86 V, 510 mA cm^{-2}).
2. Optimizing the filled state of zinc pellets and decreasing contact resistance can improve the fuel cell performance significantly. Developing surface conductive air cathode is particularly important for ZAFC.
3. Location of the cell, flow state of electrolyte and air are main factors affecting the performance and uniformity of ZAFC stack.
4. Time needed for voltage to reach steady state responding to both current step-up and current step-down are in milliseconds. Therefore, ZAFC is excellently applicable to automotive application.

Acknowledgments

The National Basic Research Program of China (973 Program) (2012CB215500), 863 Programs (2012AA110601, 2012AA053402), and the Specialized Research Fund for the Doctoral Program of

Higher Education (20090002110074) are gratefully acknowledged for funding this work.

References

[1] X.G. Zhang, Corrosion and Electrochemistry of Zinc, Plenum Publisher, 1996.
[2] D. Linden, D.B. Reddy, Handbook of Batteries, third ed., McGraw Hill, New York, NY, 2002.
[3] C.W. Lee, K. Sathiyanarayanan, S.W. Eom, H.S. Kim, M.S. Yun, J. Power Sources 160 (2006) 161–164.
[4] X.G. Zhang, ECS Trans. 16 (34) (2009) 47–59.
[5] A.A. Mohamad, J. Power Sources 159 (2006) 752–757.
[6] S.M. LLER, O. Haas, C. Schlatter, C. Comninellis, J. Appl. Electrochem. 28 (1998) 305–310.
[7] Mike C. Cheiky, Len G. Danczyk, Michel C. Wehrey, SAE papers 901516.
[8] N. Shaigan, W. Qu, T. Takeda, ECS Trans. 28 (32) (2010) 35–44.
[9] J. Goldstein, I. Brown, B. Koretz, J. Power Sources 80 (1999) 171–179.
[10] P. Sapkota, H. Kim, J. Ind. Eng. Chem. 15 (2009) 445–450.
[11] V. Neburchilov, H. Wang, J.J. Martin, W. Qu, J. Power Sources 195 (2010) 1271–1291.
[12] S.I. Smedley, X.G. Zhang, J. Power Sources 165 (2007) 897–904.
[13] J.F. Drillet, M. Adam, S. Barg, A. Herter, D. Koch, V.M. Schmidt, M. Wilhelm, ECS Trans. 28 (32) (2010) 13–24.
[14] B. Li, H. Li, J. Ma, H. Wang, J. Automotive Saf. Energy 1 (2010) 260–269.
[15] Z. Chen, J. Choi, H. Wang, H. Li, Z. Chen, J. Power Sources 196 (2011) 3673–3677.
[16] V. Jiricny, S. Siu, A. Roy, J.W. Evans, J. Appl. Electrochem. 30 (2000) 647–656.
[17] P. Sapkota, H. Kim, J. Ind. Eng. Chem. 16 (2010) 39–44.
[18] J. Han, N. Li, T. Zhang, J. Power Sources 193 (2009) 885–889.
[19] W. Chao, C. Lee, S. Shieu, C. Chou, F. Shieu, J. Power Sources 177 (2008) 637–642.
[20] J. Jang, H. Chiu, W. Yan, W. Sun, J. Power Sources 180 (2008) 476–483.
[21] W.H. Zhu, R.U. Payne, D.R. Cahela, B.J. Tatarchuk, J. Power Sources 128 (2004) 231–238.
[22] T. Mennola, M. Mikkola, M. Noponen, T. Hottinen, P. Lund, J. Power Sources 112 (2002) 261–272.
[23] A. Abrams, J. Petrol. Technol. 29 (1977) 586–592.
[24] Y. Hou, Z. Yang, X. Fang, Renew. Energy 36 (2011) 325–329.
[25] Y. Tang, W. Yuan, M. Pan, Z. Li, G. Chen, Y. Li, Appl. Energy 87 (2010) 1410–1417.